LBL-19057

Lawrence Berkeley Laboratory
UNIVERSITY OF CALIFORNIA

LBL--19057

DE85 008443

Presented at the 7th High Energy Heavy Ion Study,
GSI, Darmstadt, FRG, October 8-13, 1984

TWO PARTICLE CORRELATIONS FROM RELATIVISTIC NUCLEAR COLLISIONS

H. Wieman, K.G.R. Doss, H.A. Gustafsson,
H.H. Gutbrod, B. Kolb, H. Löhner, B. Ludewigt,
A.M. Poskanzer, T. Renner, H.G. Ritter,
and A. Warwick

January 1985

Prepared for the U.S. Department of Energy under Contract DE-AC03-76SF00098

Two Particle Correlations from Relativistic Nuclear Collisions

H.Wieman, K.G.R.Doss, H.A.Gustafsson, H.H.Gutbrod,
B.Kolb, H.Löhner, B.Ludewigt, A.M.Poskanzer, T.Renner,
H.G.Ritter and A.Warwick

Gesellschaft für Schwerionenforschung, Darmstadt, West Germany
and
Nuclear Science Division, Lawrence Berkeley Laboratory,
University of California, Berkeley, CA 94720

Abstract

Two particle correlations at low relative momentum have been examined using the Plastic Ball detector for the system 400 MeV/nucleon Ca + Ca. The unbound ^{5}Li ground state yield has been extracted from the p-^{4}He correlation and compared with a Chemical Equilibrium model along with the yield of light bound clusters. Source-size radii were measured for both Ca + Ca and Nb + Nb, at 400 MeV/nucleon from p-p correlations. The radii were found to have a cube-root dependence on the proton multiplicity of the event and the deduced thermal freezeout density was found to be about 25% of normal nuclear matter density.

Introduction

A goal in studying relativistic heavy ion collisions is to learn about nuclear matter far from conditions of normal temperature and density. Two particle correlations are a significant feature of these reactions and are therefore a potential source of information. We have looked with the Plastic Ball 4π detector for correlations between p,d,t,^{3}He and ^{4}He, and have found a number of easily observable correlations with low relative kinetic energies (0.1 to 10 MeV). This is the energy region of low lying unbound nuclear resonances. These correlations provide direct information about the late stage of the reaction where nuclear matter is highly excited and diffuse. Direct information about the early dense stage is lost since these correlations cannot be expected to survive the rigors of the initial violent dense stage. The late diffuse stage is, none the less, still far from normal unexcited nuclear matter and worthy of further study. Also there is hope that some information from the early stage can be retrieved. For instance, it is believed that entropy is preserved during expansion.

Two approaches have been taken in understanding these correlations.

One approach makes use of the density matrix formalism to generate correlation functions. The ingredients in this method are the potentials acting between the two particles which along with the appropriate boson or fermi statistics describes the final state interaction or unbound resonances. Comparison of theory with measured

MASTER

correlations yields size and temporal information about the source. This method is related to the Hanbury-Brown Twiss pion-pion interferometry type measurements of source sizes where the correlation results from boson statistics. A number of people have derived correlation functions using this approach. Koonin provided the first p-p correlation functions including final state interactions[1], and these have been widely used to extract size information[2,3,4]. Sato and Yazaki[5] using much the same approach have generated correlations for n-p,α-α,and p-p. Recently Chitwood, Lynch, Boal et al have used this approach with d-d correlations to extract source sizes for ^{16}O + Au at 25 MeV/nucleon [6]. This approach, however, is not limited to unbound pairs; it may also be applied to stronger correlations such as bound deuterons in which case it is the coalescence model. Source sizes have been extracted from deuteron yields using the Remler and Gyulassy[7] or Sato and Yazaki[8] formulation of this approach as was described earlier in this conference by H. Gustafsson[9].

A second approach to two particle correlations has been to treat them strictly as unbound resonances and determine the population of the resonance with chemical equilibrium models or other statistical models. Bernstien et al[10] have shown that the correlation function for p-p obtained in ^{16}O + ^{12}C at 25 MeV/nucleon can be reproduced by the emission and decay of ^2He. It would seem that the situation is the same here as with bound cluster production where one can use either the coalescence model or chemical equilibrium models to describe the process. Concerns have been expressed, however, that final state interactions are somehow a distinct process separate from the emission of unbound composites that later decay. In any case, ignoring this problem, it is important to test the statistical models with correlation data. Earlier this week H. Gustafsson presented entropy determinations[9] using d/p ratios in conjunction with the Quantum Statistical Model (QSM) of H. Stöcker et al[11]. Since this model at the same time predicts yields for many bound clusters and unbound nuclear resonances the consistency of this approach can be checked with the yield of unbound nuclear resonances observed in the two particle correlation measurements.

Experimental Determination of Correlations

The Plastic Ball detector[12] system used for these measurements is composed of 815 scintillator $\Delta E, E$ detector modules which cover the full solid angle region surrounding the target from 9 to 160 degrees. The lighter particles (p,d,t,^3He and ^4He) stopping in the ball detector modules are identified by their $\Delta E, E$ signatures. Only these particles with well identified energy and particle type are used for generating the pair correlations. The energy window for these well specified particles (set by the dynamic range of the $\Delta E, E$ telescopes) is from $\approx$40 to $\approx$170 MeV/nucleon. Information about other particles, however, such as energetic protons not stopped in the Ball detectors and forward angle particles, are all counted to provide further information about the collision. As will be discussed later this is important for determining the freezeout density.

Correlation functions were generated for each kind of pair as a function of relative momentum, Δp, where Δp is the momentum of one of the particles in the center of mass of the pair. Non-relativistically $\Delta p = | p_1 - p_2 | /2$ for identical particles. For comparison with expected resonances in unbound systems

$$\Delta p = \sqrt{\frac{2(m_1 + m_2)}{m_1 m_2}(E_x - Q)}$$

where E_x is the excitation energy and Q is the Q value for the ground state. The masses of the two particles in the pair are give by m_1 and m_2. Again, this is a non-relativistic expression. Formally the correlation function is

$$F = \frac{\sigma_{reaction} d^2\sigma_{12}/dp_1 dp_2}{(d\sigma_1/dp_1)(d\sigma_2/dp_2)}$$

but in practice, the correlation function is obtained by summing pairs, event by event, in bins $[N_{true}(\Delta p)]$ according to Δp, and dividing by pairs formed from particles taken from different events $[N_{mixed}(\Delta p)]$ to give

$$F(\Delta p) = norm \times N_{true}(\Delta p)/N_{mixed}(\Delta p).$$

In forming the mixed-pair sums both particles in the same detector module are rejected to be consistent with the ball's requirement of two different modules for true pairs.

Some Observed Two Particle Correlations

We observe positive correlations at small Δp in the majority of possible pairs that can be made from p,d,t,^{3}He and ^{4}He. The most striking correlations occur for pairs with Q values that reach known low lying unbound resonances. Two examples are shown in figures 1 and 2. The first example, p-^{4}He, shows a strong enhancement at the expected location for the ^{5}Li ground state. The correlation function for d-^{4}He is shown in the second figure along with the expected positions for the three lowest lying levels in ^{6}Li that decay by d-^{4}He. The lowest level shows up most clearly and the next two levels appear as a side shoulder. There are also two cases (d-d and p-d) where strong anti-correlations are observed; these are shown in figures 3 and 4. The anti-correlation which appears most strongly in our d-d spectra has also been observed by Lynch et al[6] in lower energy reactions. Boal et al have exploited this anti-correlation in the same spirit as the p-p correlations to extract source size radii[13].

Yield of ^{5}Li Ground State

We now consider in more detail the strong correlation observed in the p-^{4}He pairs corresponding to the ^{5}Li ground state. A measure of the ^{5}Li ground state yield was obtained by subtracting the non-correlated mixed pair spectrum from the true correlated pair spectrum. Before subtraction the background spectrum was normalized to the true spectrum in the region from Δp =150 MeV/c to Δp =260 MeV/c, somewhat above the ^{5}Li resonance region. This ^{5}Li yield was then corrected for the efficiency of the Plastic Ball detector. To estimate this efficiency it was necessary to make some assumptions about the angle and energy distribution of the emitted ^{5}Li. A Monte Carlo calculation of the detector acceptance was made using isotropically emitted ^{5}Li from a moving thermal source. With source velocities near the center of mass velocity the efficiency for detecting the p-^{4}He pair is 39%. The temperature used for the ^{5}Li energy spectrum was varied between 25 and 75 MeV with little effect on the efficiency. For source velocities equal to zero and the projectile velocity the efficiency drops to zero; in the first case because the ^{4}He is below the energy threshold and in the second case because the particles are confined to a small forward cone well below the 9 degree forward angle limit of the ball. The Plastic Ball detector is sensitive to ^{5}Li emitted from the participant region but not from the spectator residues.

Having obtained the ^{5}Li yield from p-^{4}He correlations and correcting for efficiency as discussed the ratio of the number of ^{5}Li divided by the number of participant protons is displayed in fig. 5. In addition, the ratio of bound fragment yields to participant proton yields are shown as a function of total participant protons in the event (including protons bound in light clusters). This total participant proton number will subsequently be referred to simply as proton multiplicity. The yield of clusters relative to protons show a clear trend of increasing with proton multiplicity. That is, the relative yield for clusters increases as the collisions become more central with increased amounts of nuclear matter in the participant or overlap region. The curves appear to be approaching a saturation value which can be compared with chemical equilibrium model fragment yields for infinite nuclear matter. In the figure we show the results of the Quantum Statistical Model (QSM) of H. Stöcker et al [11] where the entropy, the controlling parameter of this model, has been chosen to give plausible extrapolated yields for the bound clusters shown. At this point it is difficult to directly compare our ^{5}Li value with the QSM prediction shown since the measured yield was averaged over proton multiplicity values. Future analysis will rectify this problem, but we can anticipate a dependence of ^{5}Li yield on proton multiplicity similar to the bound clusters shown. In this case the QSM would appear to do as well describing the unbound ^{5}Li yield as the bound clusters. It is of interest in the future to pursue these comparisons in more detail since the QSM is a promising tool for measuring entropy (see contribution of H. Gustafsson, in this proceedings [9]).

Freezeout Density

Turning now to a different application of two particle correlations we report on the extraction of a freezeout density[4]. A hot zone of participant nucleons is created in a relativistic nuclear collision which radiates particles and clusters as it expands and cools. A size for this participant region is obtained from two particle correlations. This measured size corresponds to the stage in the expansion where, in an average sense, interactions between the particles have ceased. The thermal freezeout density is then determined by comparing this size with a count of the participant particles. For this purpose p-p correlation functions were generated as a function of Δp in much the same fashion as discussed earlier in this presentation.

In this case, however, rather than including all events together the analysis was done with groups of events separated according to proton multiplicity and, in addition, the measured p-p correlations have been normalized to unity in the region $\Delta p =$ 70-100 MeV/c. Radii have been extracted by comparing the measured correlation functions to theoretical predictions which depend on the source size radius.

The theoretical correlation functions which we compare with our measurements were calculated by Koonin[1]. In the form used here the correlation function, $F(\Delta p)$, equals $1 + R(\Delta p)$ where $R(\Delta p)$ is the correlation function of ref.[1]. The degree of correlation between the two protons is strongest when they are close in space, time and momentum. In the general form of Koonin's calculation the proton source density is treated as isotropic with a Gaussian distribution in space and time, and the proton momenta are assumed to be independent of position. The Gaussian spacial density, $\rho(r) = exp[(-r/r_g)^2]$, may be thought of as representing the proton positions at the point of their last scattering. For our analysis we assume that the time parameter is zero, ie all the protons are emitted at the same time. Consequently, our extracted radii are expected to be somewhat larger than the true spacial extent of the source. This simplified form of the correlation function (shown in fig. 6) illustrates the effects of the final state interactions between the two protons. At Δp=0 the correlation function is zero due to the Coulomb repulsion. The peak in the correlation function at Δp= 20 MeV/c is generated by the attractive nuclear force. The amplitude of this enhanced correlation is strongly dependent on the source-size parameter r_g and increases as the source gets smaller. The peak, in this case for identical fermions, is suppressed by roughly a factor of two due to Pauli exclusion. This suppression corresponds to the enhancement observed for identical bosons, the normal second order interferometry effect in pion-pion correlation measurements. The problem for this work is to compare experimental and theoretical correlation functions for the purpose of extracting the source radius r_g.

The difficulty in this comparison is caused by the smearing of the measured correlation function by the finite angular resolution of the detector modules. This causes an error in Δp which differs for each pair, being dependent on the individual proton momenta. The nature of the distortion in the measured correlation function is therefore affected by the proton momentum distributions, functions that can change depending on cuts being made on the data. The problem has been solved by including the finite-angle distortion in the theoretical correlation by use of a Monte Carlo procedure. Our procedure uses the same mixed-event pairs that are used in the experimental determination of the correlation function and therefore automatically includes the correct proton momentum distributions. An example of a distorted correlation function is shown in fig. 6 along with the original undistorted function. The effect of the distortion is to move strength from low Δp to higher Δp. The added contribution at Δp around 50 MeV/c is less apparent since the effect is diluted by the larger number of counts in both numerator and denominator as Δp increases. The distorted spectrum can now be directly compared with our measured correlation function. It should be pointed out that the Plastic Ball has a reduced efficiency for detecting pairs in the low Δp region since these pairs will tend to both go into the same detector. The efficiency has been determined from the relative number of mixed event proton pairs occurring in the same module.

The efficiency decreases from 70%, in the region of the correlation peak at $\Delta p = 20$ MeV/c, to 0 as Δp goes to 0. This loss in efficiency does not affect the ratio, but the resulting drop in statistics prevents careful comparison of data and theory at low Δp below the peak in the correlation function. However, the correlation function is well determined at $\Delta p = 20$ MeV/c and above and thus gives a good measure of the radius. In fig. 7 we show an example of a measured correlation function along with the distorted theoretical correlation function. The distorted theoretical function in this case is a linear interpolation between the two bracketing predictions for r_g = 4 and 5 fm. This interpolated curve and corresponding radius of r_g=4.7 fm was obtained by a least squares fit to the measured correlation function. Measured correlations as well as the distorted theoretical functions are calculated separately for each proton multiplicity bin.

The extracted radii are shown as a function of proton multiplicity in fig. 8. The error bars represent statistical errors only. For both the Ca + Ca and Nb + Nb system the radius increases with multiplicity. These results agree with multiplicity averaged measurements of others on a similar mass system (Ar+KCl) at higher bombarding energy. The streamer chamber results of Beavis et al[14] at E/A = 1.5 GeV are the same as ours at N_p equal to 30. The measurements of Zajc et al[15] with a beam energy of E/A = 1.8 GeV are about 20% lower than our value. The proton-proton measurements with E/A = 1.8 GeV of Zarbakhsh et al[2], on the other hand, are roughly 1/2 our values. They separate their results into two multiplicity bins and contrary to our measurements they see smaller radii at larger multiplicity.

Our radii in fig. 8 are shown with a fit using the function $r_g = r_0(N_p A/Z)^{1/3}/(\frac{5}{2})^{1/2}$ where r_0 is a reduced radius (proportional to 1 divided by the density). N_p is the proton multiplicity and A/Z has been included to reflect the presence of neutrons. The extracted radii are the radius parameters for a Gaussian source distribution, so by inclusion of $(\frac{5}{2})^{1/2}$ in the above function r_0 becomes the radius parameter of an rms-equivalent sharp sphere. The value of r_0 extracted from the fits is 1.9 fm for the two systems studied. Comparing this directly with r_0=1.2 fm, the sharp sphere r_0 for normal nuclear matter, yields a participant region freezeout density about 25% of normal nuclear density.

Comparing this value of the freezeout density with determinations by other means it is clear that different probes of the source size are sensitive to different features of the reaction. We have also measured a freezeout density using the d/p ratio in conjunction with a generalized coalescence model (reported earlier in this conference by H. Gustafsson[9]) and found a somewhat higher density. The d/p extracted densities were between 0.5 and 1.0 times normal nuclear matter density. This could be interpreted as a difference between thermal and chemical freeze out. The deuteron yield becomes fixed at a relatively high density. As the system expands the deuterons and other particles could undergo further gentle collisions which do not change the population of protons and deuterons. On the other hand, the more fragile p-p correlations would be disrupted by these gentile collisions. Only p-p correlations determined by the last scattering would survive to be measured, thus yielding a relatively low measured density. The freezeout density obtained from our measure of d-d correlations is still lower. This measurement, also reported in this conference[13], was obtained by comparing our observed d-d correlations with the radius dependent theoretical calculations of Boal et al. The calculation followed the same prescription as Koonin's for p-p correlations. The density obtained is very preliminary and can be expected to change upward when the finite angle resolution of the detector is folded in as was done for the p-p density determination. The preliminary d-d derived value, 0.09 times normal nuclear matter density, is significantly lower than the 0.25 p-p value, but this lower density, ie larger radius, has been explained by D. Boal in terms of an increased cross section for disrupting the correlation. In his analysis rms radii for last scattering were extracted in a cascade calculation for both p-p and d-d correlations. The last scattering radii in the first case was determined by the n p reaction cross section and in the second case by the larger n d reaction cross section.

Conclusion

We have looked at two particle correlations in the low relative momentum region both from the point of view of the chemical equilibrium model and from the point of view of final state interactions. Although some of our results are preliminary the chemical equilibrium model appears to give a reasonable strength for the one strong resonance we have examined, ^{5}Li ground state by p-^{4}He, as well as for the light bound clusters. The shape of the two particle correlation functions, however, contain more information than just resonance strength and the Koonin type final state interaction models with details of the particle-particle interactions in the outgoing pair are required to duplicate the measured correlation functions; particularly for the cases d-d and p-d where there is no resonance but, instead, a strong anti-correlation. The source radii and corresponding freezeout densities extracted both by two particle correlations and by the very similar d/p type analysis differ but in an expected manner. A more exacting analyses of available data and more detailed theoretical calculations like those of Boal's[13] for chemical and thermal freezeout densities are required to test this approach more quantitatively. Likewise, further work is required to truly test the chemical equilibrium model. One could expect deficiencies to appear under closer scrutiny since these models start with a minimum of complexity but results so far encourage using the chemical equilibrium model as a tool for measuring entropy.

Acknowledgments

We are grateful for the continuous support of Prof. R. Bock. This work was supported in part by the Director, Office of Energy Research, Division of Nuclear Physics of the Office of High Energy and Nuclear Physics of the U.S. Department of Energy under Contract DE-AC03-76SF00098.

REFERENCES

1. S.E. Koonin, Phys. Lett. 70B,43(1977).
2. F. Zarbakhsh, A.L. Sagle, F. Brochard, T.A. Mulera, V. Perez-Mendez,

R. Talaga, I. Tanihata, J.B. Carroll, K.S. Ganezer, G. Igo, J. Oostens, D. Woodard, and R. Sutter, Phys. Rev. Lett. 46,1268(1981).

3. W.G. Lynch, C.B. Chitwood, M.B. Tsang, D.J. Fields, D.R. Klesch, C.K. Gelbke, G.R. Young, T.C. Awes, R.L. Ferguson, F.E. Obershain, F. Plasil, R.L. Robinson and A.D. Panagiotou, Phys. Rev. Lett. 51,1850(1983).

4. H.A. Gustafsson, H.H. Gutbrod, B. Kolb, H. Löhner, B. Ludewigt, A.M. Poskanzer, T. Renner, H. Riedesel, H.G. Ritter, A. Warwick, F. Weik and H. Wieman, Phys Rev. Lett. 53,544(1984).

5. H. Sato and K. Yazaki, Proceedings of the Hakone Seminar, 1,340(1980)

6. C.B. Chitwood et al., Michigan State University Cyclotron Laboratory Report (1984).

7. M. Gyulassy and E. Remler to be published.

8. H. Sato and K. Yazaki, Phys. Lett. 98B,153(1981).

9. H.A. Gustafsson, Proceedings this Conference

10. M.A. Bernstein, W.A. Friedman, W.G. Lynch, C.B. Chitwood, D.J. Fields, C.K. Gelbke, M.B. Tsang, T.C. Awes, R.L. Ferguson, F.E. Obershain, F. Plasil, R.L. Robinson and G.R. Young, Michigan State University Cyclotron Laboratory Report MSUCL-494.

11. H. Stöcker, G. Buchwald, G. Graebner, P.Subramanian, J.A. Maruhn, W. Greiner, B.V. Jacak and G.D. Westfall, Nucl. Phys. A400,63(1983).

12. A. Baden, H.H. Gutbrod, H. Löhner, M.R. Maier, A.M. Poskanzer, T. Renner, H. Riedesel, H.G. Ritter, H. Spieler, A. Warwick, F. Weik and H. Wieman, Nucl. Instr. and Meth. 203,189(1982).

13. D.H. Boal, Proceedings this Conference

14. D. Beavis, S.Y. Fung, W. Gorn, A. Huie, D. Keane, J.J. Lu, R.T. Poe, B.C. Shen, and G. VanDalen, Phys. Rev. 27C,910(1983).

15. W.A. Zajc, J.A. Bistirlich, R.R. Bossingham, H.R. Bowman, C.W. Clawson, K.M. Crowe, K.A. Frankel, J.G. Ingersoll, J.M. Kurck, C.J. Martoff, D.L. Murphy, J.O. Rasmussen, J.P. Sullivan, E. Yoo, O. Hashimoto, M. Koike, W.J. McDonald, J.P. Miller and P. Truol, Phys. Rev. 29C,2173(1984)

Figure captions

1. The measured p-^{4}He correlation function for Ca + Ca at 400 MeV/nucleon. The expected position for the ^{5}Li ground state is marked.
2. The measured d-^{4}He correlation function for Ca + Ca at 400 MeV/nucleon. The expected position for the first three levels in ^{6}Li which decay by d-^{4}He are indicated.
3. The measured d-d correlation function for Ca + Ca at 400 MeV/nucleon.
4. The measured p-d correlation function for Ca + Ca at 400 MeV/nucleon.
5. The yields of bound clusters d,t,^{3}He and ^{4}He divided by the number of unbound participant protons are shown as a function N_p, the total number

of participant protons (bound and unbound). Also shown is the yield of the unbound ^{5}Li ground state divided by the number of unbound participant protons. This point is shown at the mean N_p value for the sample studied. The corresponding ratios from the Quantum Statistical Model of H. Stöcker et al[11] are indicated at the right.

6. The solid curve shows the p-p correlation function calculated by Koonin for a source of radius r_g=3 fm and a source life time of $\tau = 0$. The dashed curve is the same correlation after applying the Plastic Ball distortion resulting from finite angular granularity.

7. The measured p-p correlation function for Ca + Ca at 400 MeV/nucleon events with a proton multiplicity from 25 to 32. The solid curve is a least squares fit interpolation between distorted theoretical correlation functions for radii of 4 and 5 fm.

8. Extracted Gaussian source radii as a function of proton multiplicity (N_p) for the two systems Ca + Ca and Nb + Nb at 400 MeV/nucleon. The curves are fits to the results with the function, $r_g = r_0(N_p A/Z)^{1/3}/(\frac{5}{2})^{1/2}$.

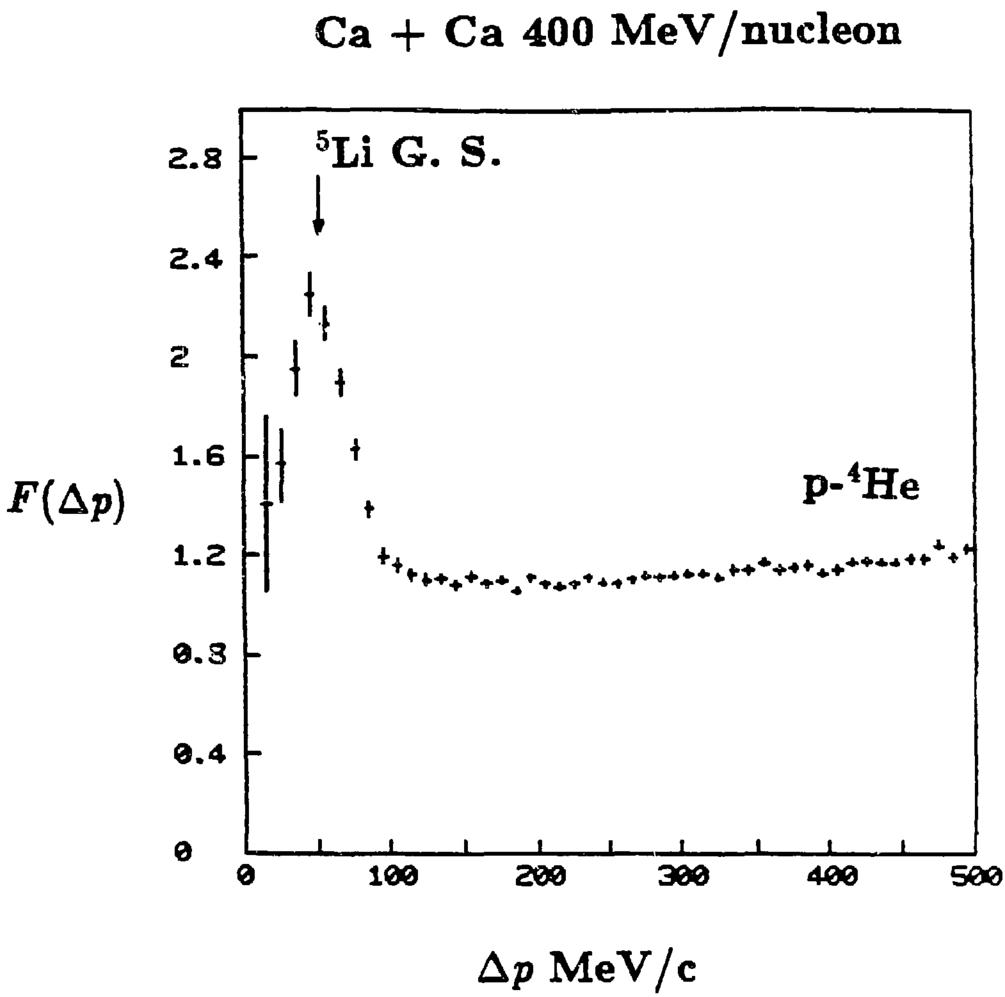
Ca + Ca 400 MeV/nucleon
^{5}Li G. S.
p-^{4}He
$F(\Delta p)$
2.8
2.4
2
1.6
1.2
0.8
0.4
0
0
100
200
300
400
500
Δp MeV/c

Figure 1

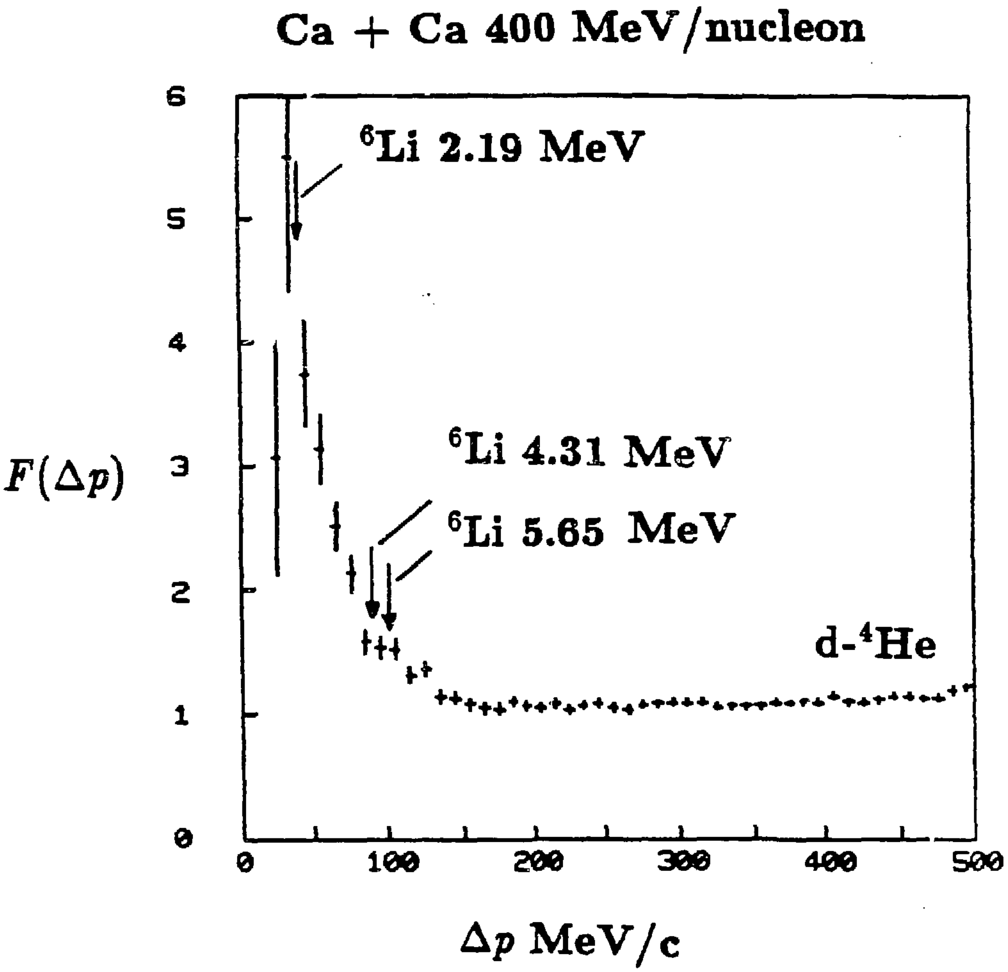

Ca + Ca 400 MeV/nucleon
6
5
4
3
2
1
0
$F(\Delta p)$
^{6}Li 2.19 MeV
^{6}Li 4.31 MeV
^{6}Li 5.65 MeV
d-^{4}He
0
100
200
300
400
500
Δp MeV/c

Figure 2

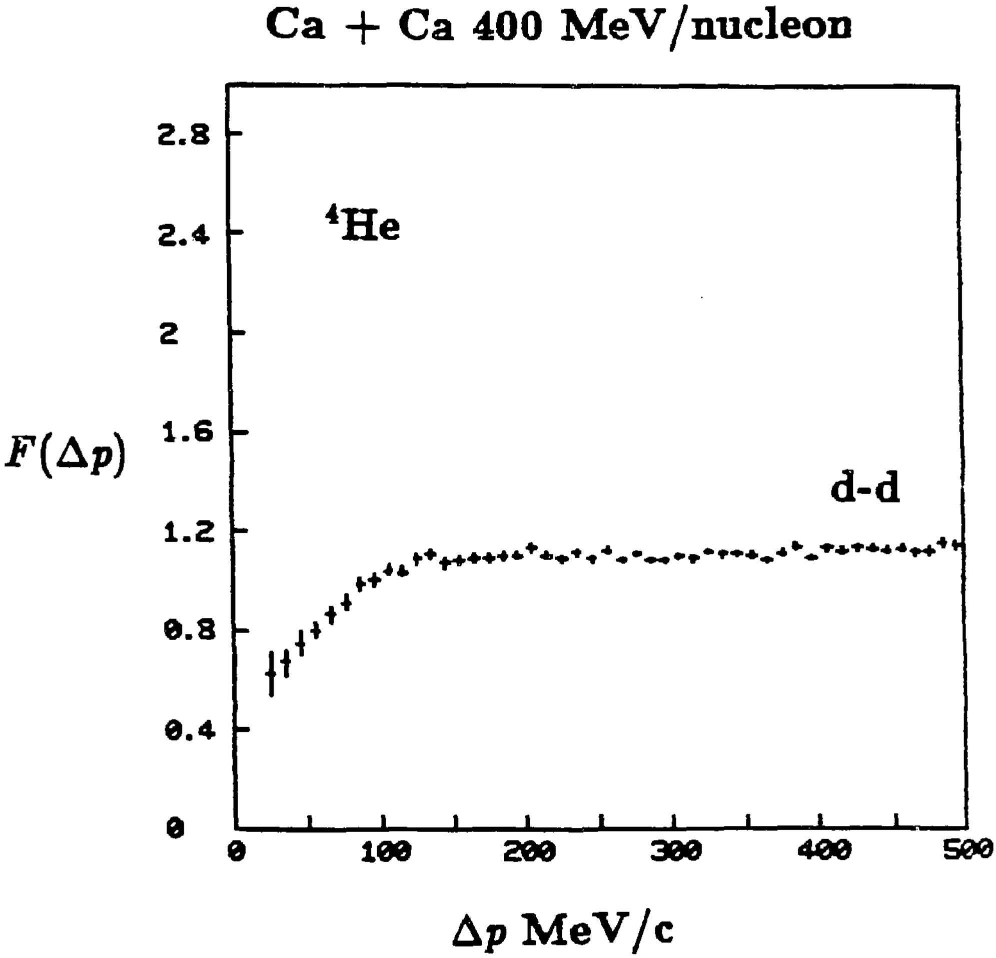
Ca + Ca 400 MeV/nucleon
^{4}He
d-d
$F(\Delta p)$
2.8
2.4
2
1.6
1.2
0.8
0.4
0
0
100
200
300
400
500
Δp MeV/c

Figure 3

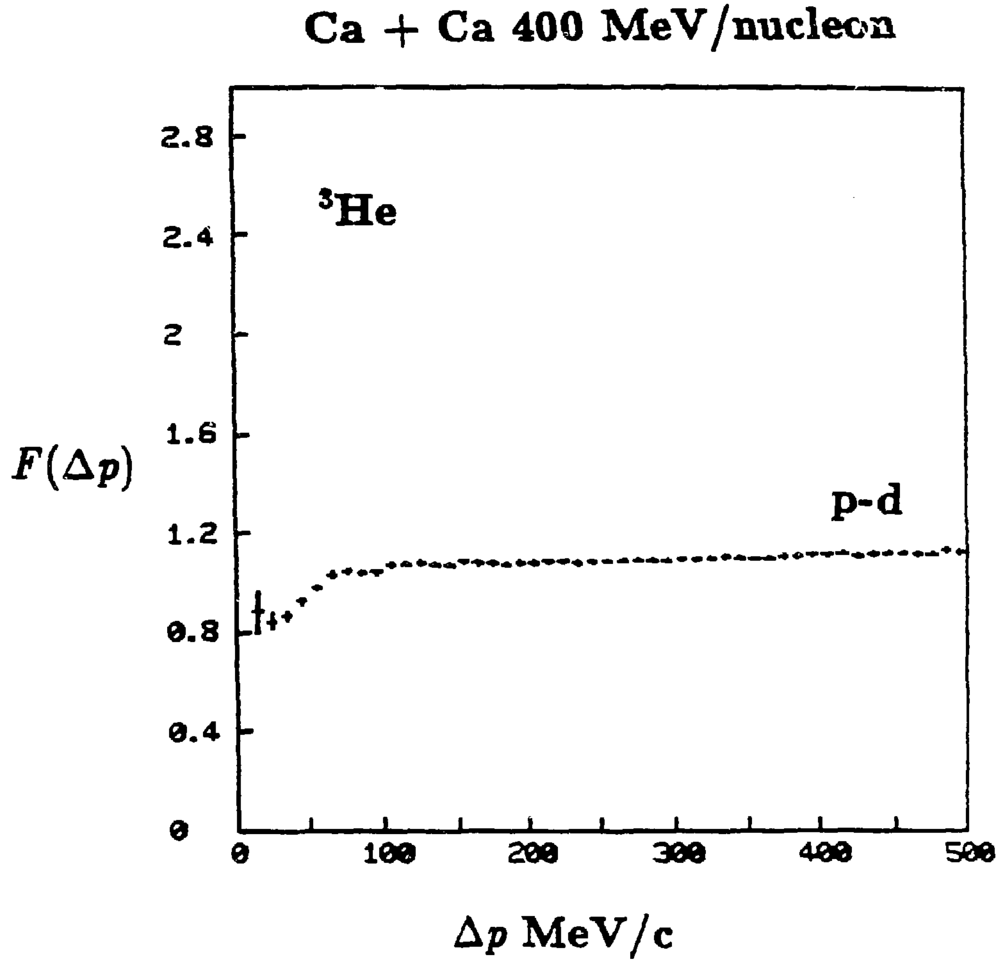
Ca + Ca 400 MeV/nucleon
^{3}He
p-d
$F(\Delta p)$
2.8
2.4
2
1.6
1.2
0.8
0.4
0
100
200
300
400
500
Δp MeV/c

Figure 4

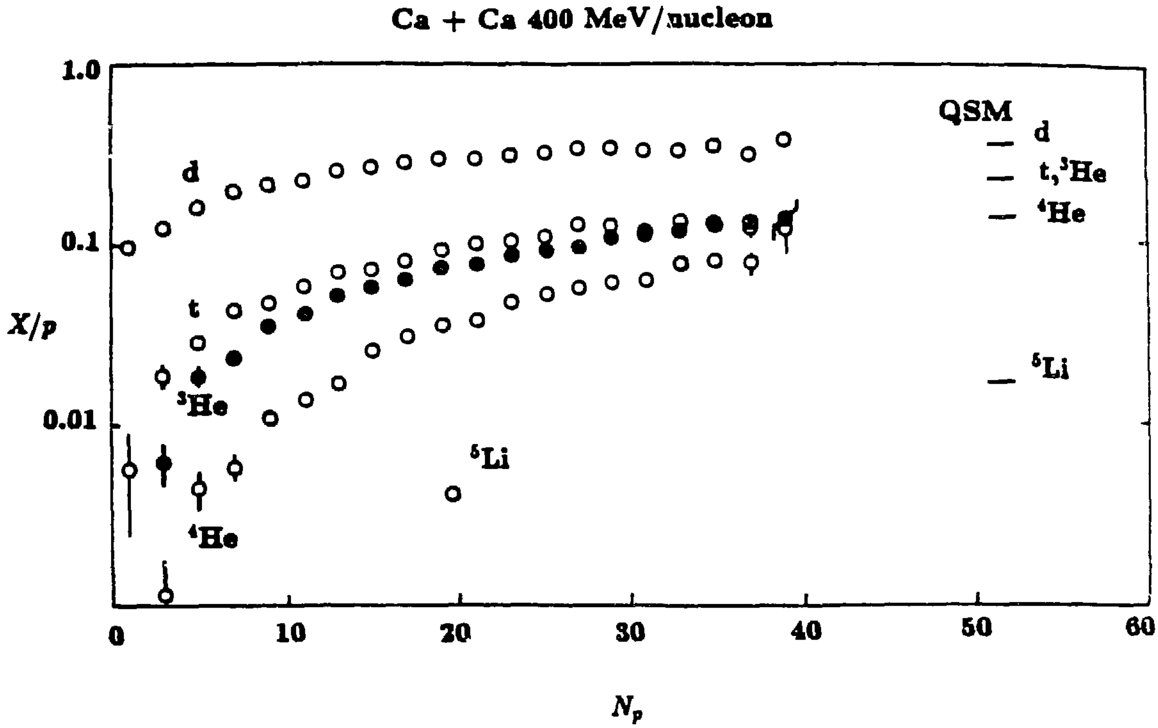

Ca + Ca 400 MeV/nucleon
1.0
0.1
0.01
X/p
d
t
³He
⁴He
⁵Li
QSM
d
t,³He
⁴He
⁵Li
0
10
20
30
40
50
60
N_p

Figure 5

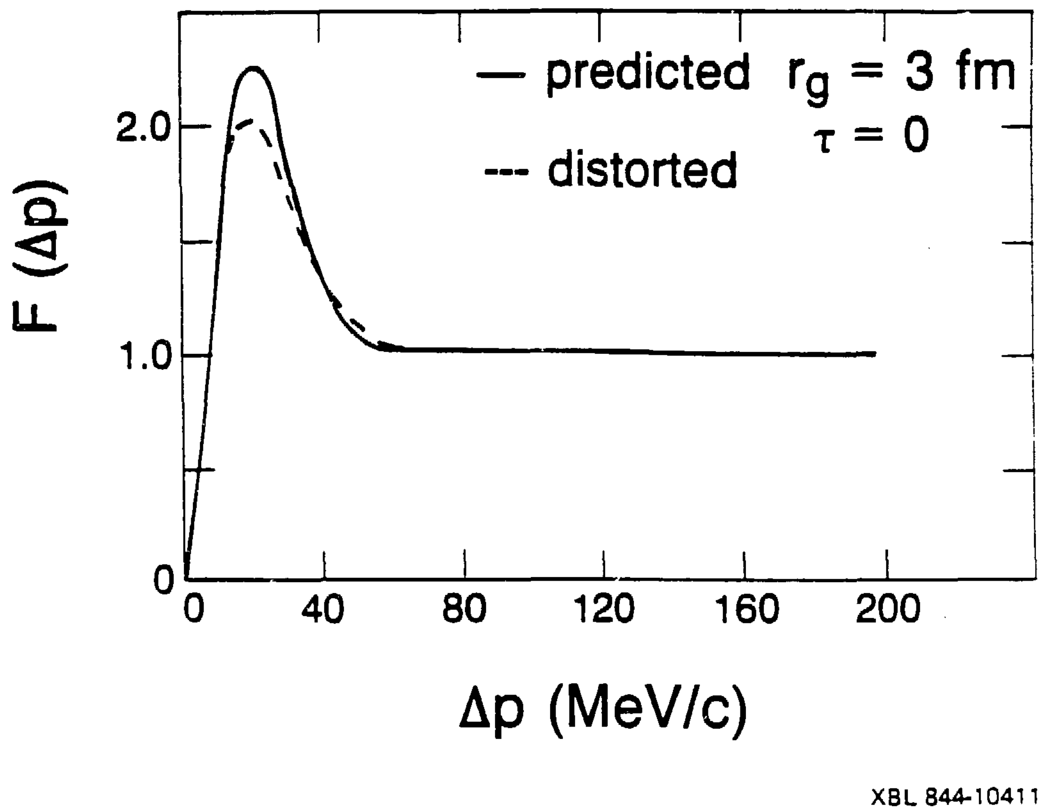

— predicted
--- distorted
r_g = 3 fm
τ = 0
F (Δp)
2.0
1.0
0
0
40
80
120
160
200
Δp (MeV/c)
XBL 844-10411

Figure 6

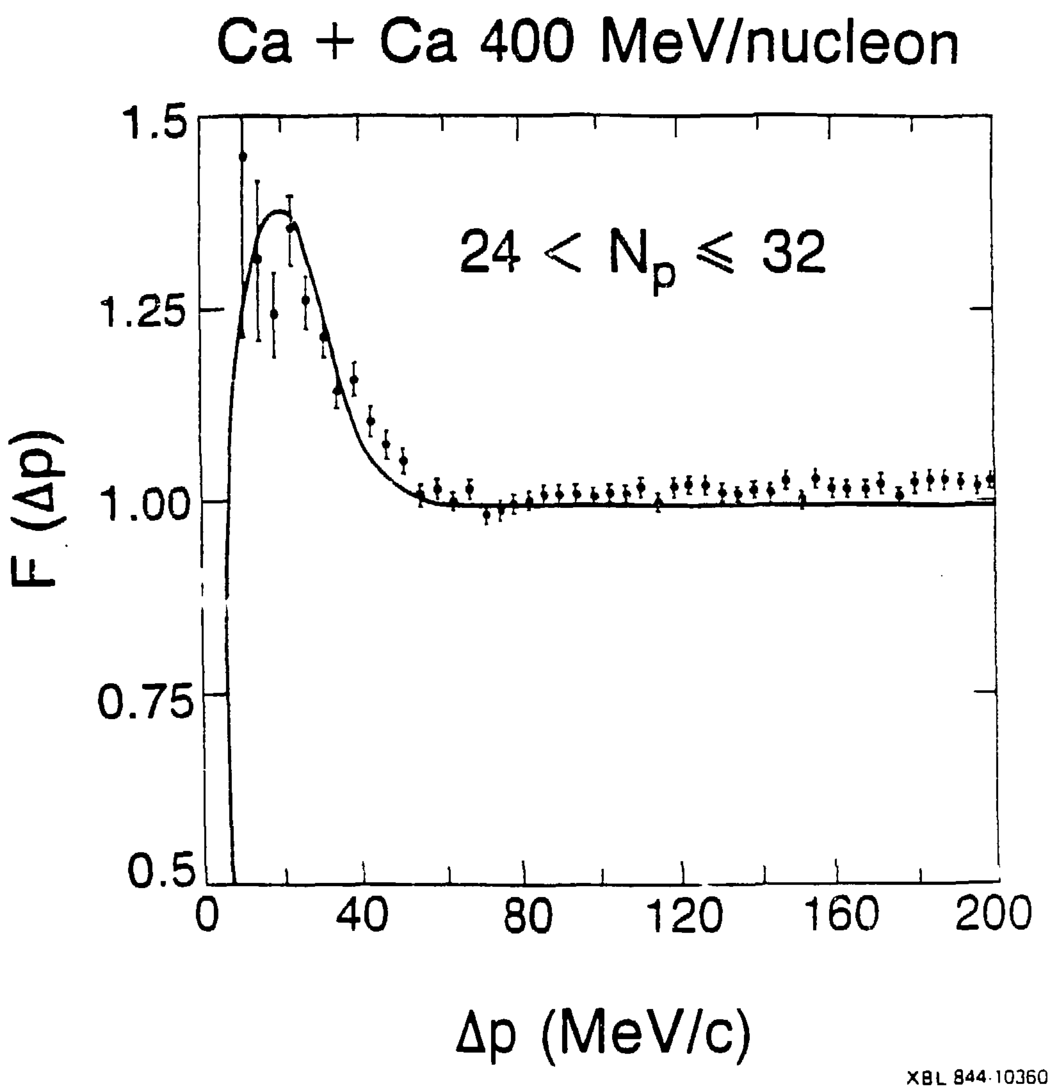
Ca + Ca 400 MeV/nucleon
1.5
1.25
1.00
0.75
0.5
F (Δp)
24 < N_p ≤ 32
0
40
80
120
160
200
Δp (MeV/c)
XBL 844-10360

Figure 7

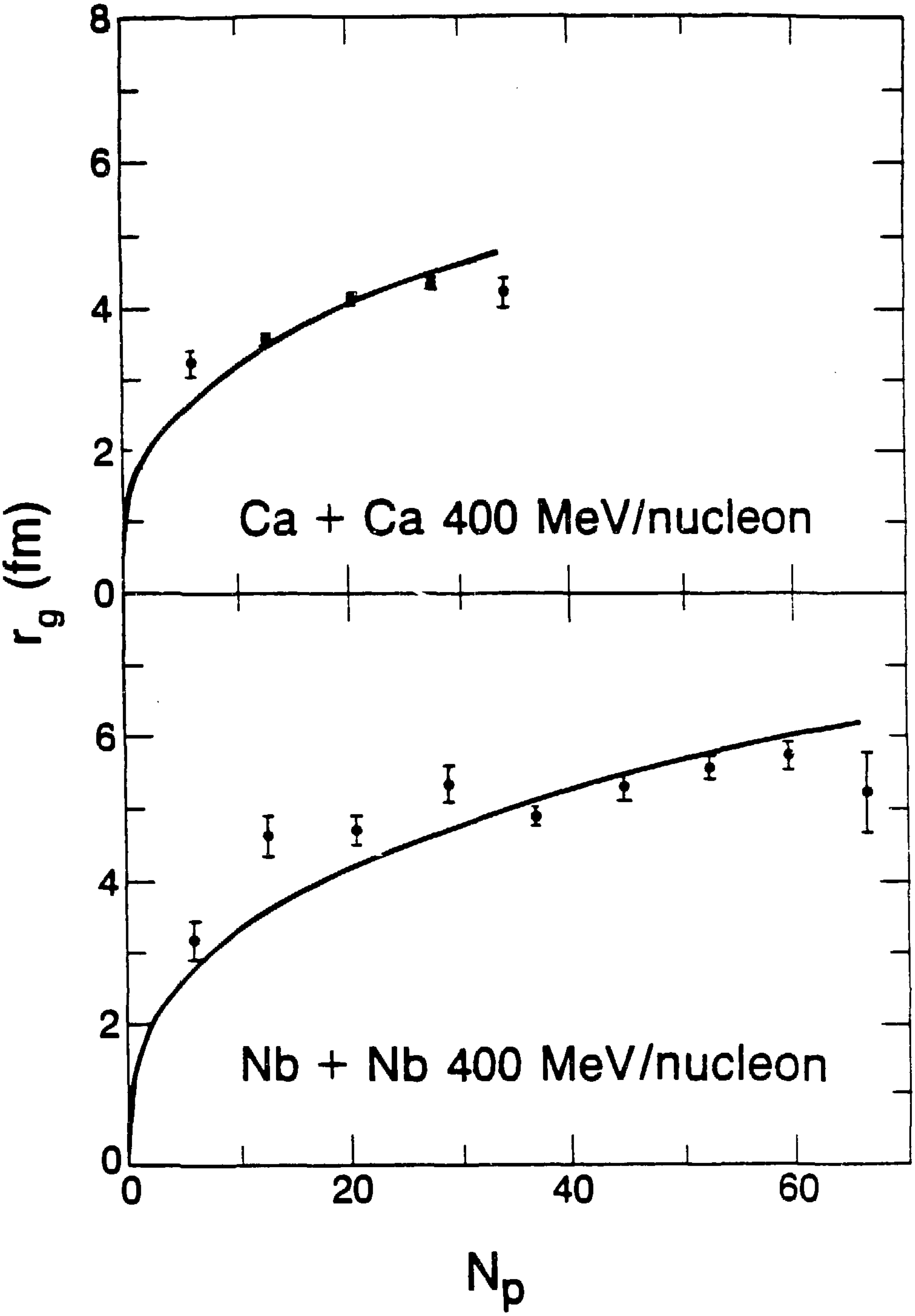

XBL 842-10058

Figure 8